

Identification of concentrations and sources of PM_{2.5}-bound PAHs in North China during haze episodes in 2013

Wei Lu² · Lingxiao Yang^{1,2} · Jianmin Chen^{1,2,3} · Xinfeng Wang¹ · Hao Li^{1,5} · Yanhong Zhu¹ · Liang Wen¹ · Caihong Xu¹ · Junmei Zhang¹ · Tong Zhu⁴ · Wenxing Wang¹

Published online: 8 December 2015
© Springer Science+Business Media Dordrecht 2015

Abstract An analysis of 12 polycyclic aromatic hydrocarbons (PAHs) in PM_{2.5} (particulate matter with a diameter smaller than 2.5 microns) samples collected at Yucheng, Shandong, in June 2013 was conducted to determine the concentrations, composition, sources, and associated cancer risk. The results revealed that the average PAH concentration was higher during haze episodes ($28.28 \pm 8.35 \text{ ng m}^{-3}$) when compared to non-haze episodes ($23.68 \pm 4.17 \text{ ng m}^{-3}$), and diagnostic ratio and principal component analyses indicate that the predominant sources of PAHs were from fossil fuel and coal combustion, likely from vehicle emissions and industrial sources and biomass burning. Coal combustion and biomass burning contributed significantly more during haze episodes, whereas liquid fossil fuel combustion (e.g. petroleum) was the dominant contributor during the non-haze periods. In addition, back-trajectory calculations revealed that the long-distance transport of air masses from regions with industrial pollution

and biomass burning contributed significantly to the concentrations of PAHs in the region. The concentration of high molecular weight PAHs (HMW-PAHs) increased from 62.3 % under non-haze conditions to 67.9 % during the haze periods. The benzo[a]pyrene-equivalent carcinogenic potency value during haze episodes was higher (7.09 ng m^{-3}) than that during non-haze (5.64 ng m^{-3}) periods and adults over 30 years old in the Shandong province are at an increased risk of cancer from PAHs.

Keywords Polycyclic aromatic hydrocarbons · Source · Haze episode

Introduction

Over the last decade, atmospheric pollution has become the most critical environmental issue in China due to the deterioration of air and water quality and human health (Wang et al. 2006; Duan et al. 2012; Xu et al. 2013a, b). Haze events are caused by high concentrations of fine particulate matter (i.e. particles with a diameter smaller than 2.5 microns, PM_{2.5}) and stable meteorological conditions (Watson 2002; Guo et al. 2003a). During January 2013, persistent haze events originating in Northern China spread at an unprecedented rate to encompass nearly the entire eastern half China, resulting in significant economic losses and a notable increase in outpatient and emergency services (Mu and Zhang 2013). It has become evident that haze events can have serious health impacts on the populace; however, the mechanisms and species responsible for the observed deterioration have yet to be elucidated. Polycyclic aromatic hydrocarbons (PAHs), toxic organic species frequently found in PM_{2.5}, have attracted significant attention due to their carcinogenic and mutagenic effects; therefore, several studies have been conducted worldwide to

✉ Lingxiao Yang
yanglingxiao@sdu.edu.cn

¹ Environment Research Institute, Shandong University, Jinan 250100, China

² School of Environmental Science and Engineering, Shandong University, Jinan 250100, China

³ Shanghai Key Laboratory of Atmospheric Particle Pollution and Prevention (LAP3), Fudan Tyndall Centre, Department of Environmental Science and Engineering, Fudan University, Shanghai 200433, China

⁴ State Key Lab for Environment Simulation and Pollution Control, College of Environmental Sciences and Engineering, Peking University, Beijing 100871, China

⁵ Henan Institute of Engineering, Zhengzhou 451191, China

quantify and identify the PAHs. Xu et al. (2013a, b) reported that 30 % of the population in China is living in regions with concentrations of PAHs that exceeded the national ambient benzo[a]pyrene standard of 10 ng m^{-3} . Furthermore, it has been reported that Chinese emissions of PAHs accounted for nearly 21 % of the total global PAH emissions in 2004 (Zhang and Tao 2009; Shen et al. 2014). The haze formation in China is unique due to the rapid transition from clean to heavily polluted conditions and because the haze events can persist for several days. Therefore, it is critical that the concentration and speciation of PAHs during polluted periods is evaluated to determine the potential effects of haze events on human health.

Haze episodes occur most frequently in North China, where the highest concentrations of PAH emissions in both urban and rural areas have also been reported (Zhang et al. 2007). Previous investigations examining the concentrations, sources, and toxicity assessment of PAHs have been conducted in heavily populated urban areas in North China, such as Beijing, Tianjin, Jinan, and Qingdao (Zhou et al. 2005; Wu et al. 2005; Zhu et al. 2015; Guo et al. 2003a, b). Previous PAH studies have generally been conducted in winter, when the $\text{PM}_{2.5}$ and PAH concentrations are the highest, and little attention has been given to the concentrations of PAHs during the warmer seasons. However, the high temperatures, humidity, and solar radiation in the summer are more favourable to the formation of secondary pollutants, and motor vehicle exhaust emissions, due to the use of car air conditioners, and biomass burning increase during the summer, which can lead to elevated concentration of PAHs. In particular, more than 140,000,000 tons of straw is burned in North China, which not only leads to heavily polluted periods but also produces high PAH concentrations in summer (Cao et al. 2008; Koe et al. 2001; Li et al. 2010; Fang et al. 1999; Yan et al. 2006; Yang et al. 2008). Although Yucheng, located in the centre of North China, is far from sources of industrial pollution, it is downwind of both the Beijing–Tianjin–Hebei region and straw burning in southeast China. Thus, this location is ideal for measurements of characteristics of PAHs in a rural area during the summer to gain a more comprehensive understanding of PAHs.

In this study, we collected $\text{PM}_{2.5}$ samples at Yucheng in June 2013 during the peak biomass burning season and then evaluated the concentration of 12 PAHs that are regulated by the United States Environmental Protection Agency (US EPA) due to their high toxicity. This study focused on four central objectives: (a) to analyse the compositional characteristics of PAHs during both haze and non-haze periods; (b) to identify the sources of PAHs using diagnostic ratios and principal component analysis (PCA); (c) to assess the cancer risk of PAHs in the rural Chinese atmosphere; and (d) to estimate the effects of long-range transport of PAHs by back-trajectory analysis.

Material and methods

Filter sampling

The measurements were conducted at Yucheng ($36^\circ 87' \text{ N}$, $116^\circ 57' \text{ E}$) in the Shandong province (Fig. 1), which was described in detail in our previous study (Wen et al. 2015). The air sampler was a medium-volume $\text{PM}_{2.5}$ sampler (TH-150A, Wuhan Tianhong Intelligence Instrument Facility, Wuhan, China), operating at 100 litres per minute (LPM). The utilized quartz filters were 88 mm in diameter with 1- μm pores (Pall Gelman Inc., USA). Before sampling, the quartz filters were baked at 600°C in a muffle furnace for 2 h, and the $\text{PM}_{2.5}$ cutting heads were cleaned with anhydrous ethanol to remove any organic compounds (Zhu et al. 2013). We collected $\text{PM}_{2.5}$ samples on non-rainy days between 1 and 30 June 2013 at Yucheng, resulting in 24 daytime and 22 nighttime samples. The sampling periods were approximately 12 h (i.e. between 8:00 and 19:30 for daytime and between 20:00 and 7:30 for nighttime). All samples were kept in a refrigerator at -20°C until analysis to avoid the volatilization of the measured materials.

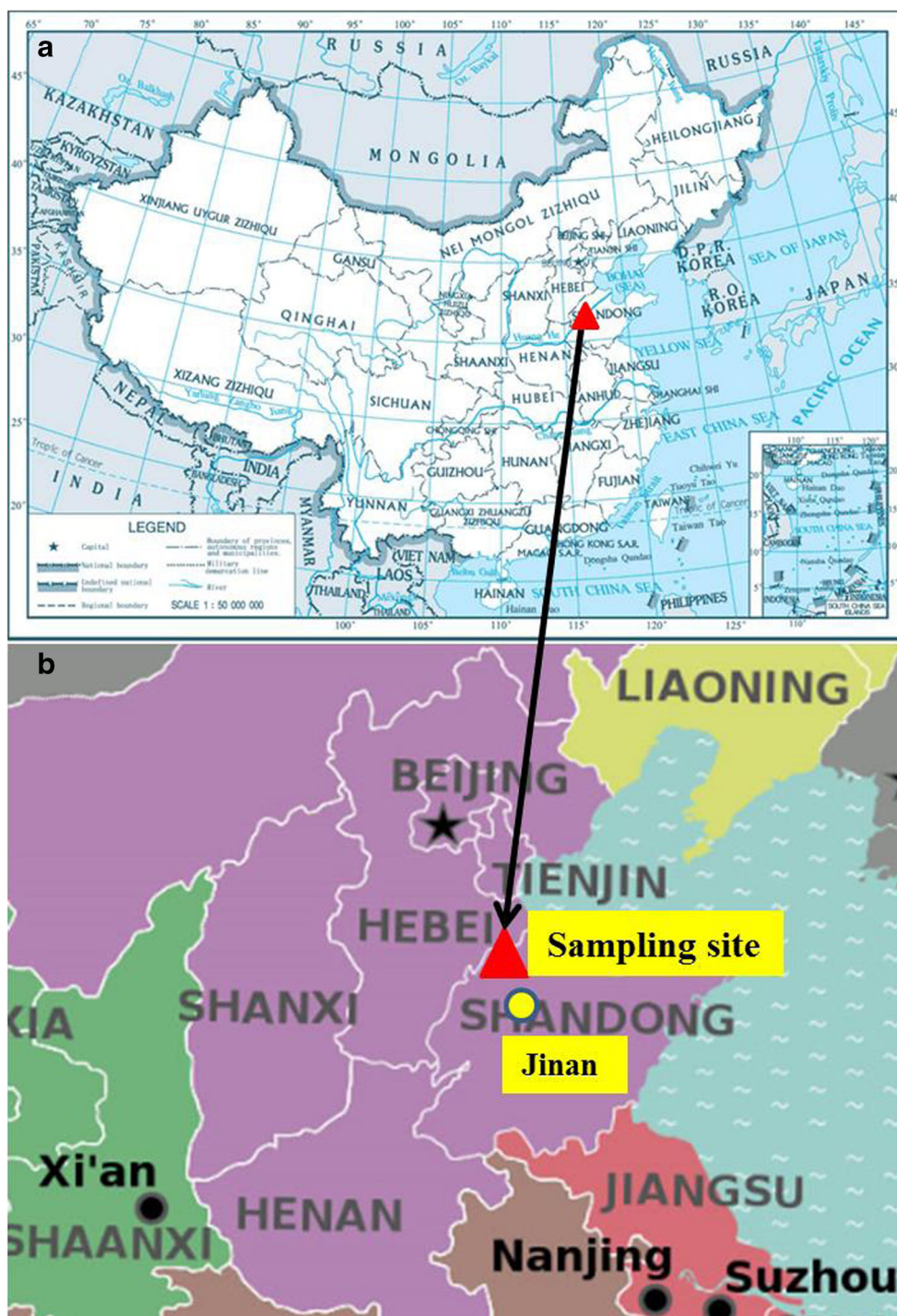
Extraction and analysis

Before and after sampling, the filters were held in an environment of constant temperature ($20 \pm 1^\circ \text{C}$) and humidity ($50 \pm 2\%$) for 24 h and then weighed on a microbalance (Model BP211D; Sartorius, Germany), which was accurate at 0.001 mg (Zhu et al. 2013). The difference between the weight before and after sampling was used to calculate the 12-h average concentrations of $\text{PM}_{2.5}$.

The specific pre-treatment procedure and process of analysing the PAHs have been described in our previous studies (Zhu et al. 2013, 2015). Briefly, three 17-mm-diameter pieces were cut from the 88-mm filters, and the PAHs were extracted by applying an acceleration solvent (ASE300, Agilent) comprised of 80 % dichloromethane (DCM) and 20 % *n*-hexane. The extracted organic were combined and concentrated on a rotary evaporator, and then the solution was reduced to about 1 ml under a gentle stream of nitrogen and finally stored in a refrigerator at -4°C until analysis.

The analysis was performed using a gas chromatograph (Agilent Technologies 6890N Network GC System Agilent Co., USA) equipped with a mass selective detector mass spectrometer (Agilent 5973 Network). A DB-5 capillary column with $30 \text{ m} \times 0.25 \text{ mm} \times 0.5 \mu\text{m}$ film thickness was applied to the separate measurements. The temperature programme for the chromatographic run was referred to Ma et al. (2010). This methodology allows us to separate the $\text{PM}_{2.5}$ samples into 16 discrete PAHs: naphthalene (Nap), acenaphthylene (Acy), acenaphthene (Ace), fluorine (Flo), phenanthrene (Phe), anthracene (Ant), fluoranthene (Flt), pyrene (Pyr),

Fig. 1 **a** The location of Yucheng (marked with a red triangle). **b** The location of our sampling site (marked with a red triangle)



benz[a]anthracene (BaA), chrysene (Chr), benzo[b]fluoranthene (BbF), benzo[k]fluoranthene (BkF), benzo[a]pyrene (BaP), indeno[1,2,3-cd]pyrene (InP), dibenz[a,h]anthracene (DbA), and benzo[ghi]perylene (BgP). In the atmosphere, Nap, Ace, Acy, and Flo preferentially exist in the vapour phase (Tan et al. 2011; Hu et al. 2012), which results in a low recovery in particulate sampling; therefore, these four PAHs were excluded from

the study. The limit of detection for the PAHs ranged from 0.005 ng m^{-3} (Ace) to 0.139 ng m^{-3} (BgP).

Quality control

Control blank field and procedural (i.e. solvent only) experiments were conducted to ensure the quality of sampling and measurement data. Procedural control experiments were

performed for every field sample to ensure that there was no significant background interference. The measured extraction recoveries ranged from 70 to 125 % for the 12 PAHs. None of the targeted PAHs were detected in the control experiments.

Cancer risk assessment

The incremental lifetime cancer risk (ILCR) quantitatively estimates the exposure risk of inhaled air particles contaminated with PAHs based on the US EPA standard model (Chen and Liao 2006; Peng et al. 2011). The unitless equation used for calculating ILCR in terms of inhalation is

$$\text{ILCR}_{\text{inhalation}} = \text{CSF}_{\text{inhalation}} \times \frac{C \times \text{IR}_{\text{inhalation}} \times \text{ED} \times \text{EF}}{\text{BW} \times \text{ALT}} \quad (1)$$

where C is the PAH concentration in air particles (ng m^{-3}), $\text{IR}_{\text{inhalation}}$ is the air inhalation rate ($\text{m}^3 \text{day}^{-1}$), EF is the exposure frequency (day year^{-1}), ED is the lifetime exposure duration (years), BW is the body weight (kg), ALT is the averaging lifetime for carcinogens (years), and $\text{CSF}_{\text{inhalation}}$ is the cancer slope factor ($\text{per mg kg}^{-1} \text{day}^{-1}$). An EF of 350 was used to calculate the lifetime dose of PAHs, signifying that the exposed group (i.e. receptors) inhales PAHs 350 days out of a year in the scenario-specific exposure pathway (Koe et al. 2001). This assumption is based on the protective estimate that all receptors spend a maximum of 2 weeks away from the exposure scenario location (USEPA 2005). A CSF value for the inhalation of BaP was assumed to be $3.14 (\text{mg kg}^{-1} \text{day}^{-1})^{-1}$ (Chen and Liao 2006). In this study, the ILCR for the total BaP equivalent carcinogenic potency (BaP_{eq}) values was determined for specific age groups (infants, toddlers, children, adolescents, and adults). The total BaP_{eq} values obtained during haze and non-haze periods were used to calculate the daily exposure level through inhalation.

Results and discussion

Concentration overview

The criteria for classifying haze and non-haze episodes were as follows: a haze day was defined as that with visibility of less than 10 km and relative humidity of less than 90 %. Non-haze days were considered to occur when the visibility exceeded 10 km and the $\text{PM}_{2.5}$ concentration was less than $75 \mu\text{g m}^{-3}$ (Ministry of Environmental Protection of The People's Republic of China 2012).

During the entire sampling period, the 12-h average concentration of $\text{PM}_{2.5}$ was $129.63 \pm 74.63 \mu\text{g m}^{-3}$, ranging from 24.87 to $339.11 \mu\text{g m}^{-3}$. During haze episodes, the average concentration of $\text{PM}_{2.5}$ was $235.84 \pm 66.39 \mu\text{g m}^{-3}$ (140.69 – $339.11 \mu\text{g m}^{-3}$), which was 3.7 times higher than the concentration observed during the non-haze episodes ($64.44 \pm$

$19.80 \mu\text{g m}^{-3}$, 24.87 – $92.45 \mu\text{g m}^{-3}$). The highest 12-h average concentration of $\text{PM}_{2.5}$ measured ($339.11 \mu\text{g m}^{-3}$) was 5 times higher than the national second grade classification (i.e. 24-h $\text{PM}_{2.5} < 75 \mu\text{g m}^{-3}$) set by the Chinese government (Ministry of Environmental Protection of The People's Republic of China 2012). The average concentration of the 12 PAHs was 28.28 ± 8.35 (range 16.66 – 45.49ng m^{-3}) and $23.68 \pm 4.17 \text{ng m}^{-3}$ (range 15.16 – 29.66ng m^{-3}) during haze episodes and clean periods, respectively (Table 1). Our measured sum of the 12 PAHs during the haze period was comparable to that measured in Taiwan (33.0ng m^{-3} for 21 PAHs) in 2010 during the rice straw burning period (Lai et al. 2009). The concentration of particulate PAHs during haze episodes in our study were found to be higher than several other rural and suburban sites, such as the Muang District in the Lampang province in Northern Thailand (5.1ng m^{-3} for 16 PAHs) and Araraquara in Brazil (11.6ng m^{-3} for 16 PAHs) (Phoothiwut et al. 2013; De Andrade et al. 2010). However, the concentration was lower than the measured values in Baofeng Country, Henan province (34.82ng m^{-3} for 16 PAHs) (Wu et al. 2015), where fossil fuels are utilized for cooking and heating, the rural fields in Taiyuan, Shanxi province (36.33ng m^{-3} for 21 PAHs), where biofuels are heavily used for heating (Li et al. 2014), and in Guangzhou (44.22ng m^{-3} for 14 PAHs) during a heavy haze period (Tan et al. 2011).

PAH compositional pattern

The 12 PAH species can be classified into low molecular weight (LMW, 3-ring PAHs), middle molecular weight (MMW, 4-ring PAHs), and high molecular weight (HMW, 5- and 6-ring PAHs) species. A higher LMW concentration represents the presence of more non-combusted petroleum products, whereas HMW species are typically related to pyrogenic products derived mainly from fossil fuel combustion (Hassanien and Abdel-Latif 2008). The average concentrations of the LMW, MMW, and HMW species were $2.38 \pm 0.58 \text{ng m}^{-3}$, $6.70 \pm 2.38 \text{ng m}^{-3}$, and $19.20 \pm 7.57 \text{ng m}^{-3}$ during haze episodes and $2.07 \pm 0.33 \text{ng m}^{-3}$, $6.93 \pm 3.25 \text{ng m}^{-3}$, and $14.68 \pm 3.29 \text{ng m}^{-3}$ during non-haze periods (Table 1). Moreover, the proportions of the LMW, MMW, and HMW species during haze (1:2.82:8.07) and non-haze episodes (1:3.3:7.1) showed that although HMW species were the main components in both haze and non-haze episodes, the proportion of HMW species increased from 62.3 % in non-haze to 67.9 % in haze conditions. The MMW species decreased from 28.9 % in non-haze to 23.7 % in haze conditions, which may be related to the different sources of the PAHs.

Sienra et al. (2005) proposed that specific PAHs are derived from combustion (COMPAHs), including Flt, Pyr, Chr, BbF, BkF, BaA, BaP, InP, and BgP. The concentration of COMPAHs measured during haze episodes was in the range of $23.3 \pm 6.49 \text{ng m}^{-3}$, accounting for 82.75 ± 2.81 % of the

Table 1 The concentrations of individual PAH compounds at Yucheng with other measurement study results (unit: ng/m³)

PAH	The whole sampling periods ^a			Haze ^a		Non-haze ^a		Guangzhou ^b	Muang District ^c	Araraquara ^d	Taiwan ^e	Taiyuan ^f	Baofeng ^h
	Range	Mean (n=46)	Range	Mean (n=11)	Range	Mean (n=14)							
Ant	0.28–1.39	0.65±0.25	0.44–1.00	0.65±0.17	0.29–1.00	0.56±0.20	0.18						
Phe	0.97–2.72	1.55±0.36	1.16–2.72	1.72±0.52	0.97–2.09	1.51±0.32	1.20						
Flt	0.80–7.21	2.93±1.57	0.91–5.54	2.46±1.24	1.03–4.10	2.41±1.10	2.56						
Pyr	0.01–15.05	3.05±3.10	0.07–3.90	1.46±1.39	0.01–4.95	3.00±1.79	2.85						
Chr	0.33–2.15	0.78±0.35	0.44–1.10	0.81±0.24	0.33–0.77	0.58±0.14	5.77						
BaA	0.96–5.83	1.99±0.96	1.13–3.62	1.97±0.71	0.96–2.26	1.58±0.39	3.29						
BkF	1.90–7.61	4.07±1.59	1.90–7.61	4.61±1.73	1.97–5.00	3.49±0.81							
BbF	0.19–6.54	2.87±1.54	1.51–6.18	3.40±1.62	0.55–3.63	2.26±0.89							
BaP	1.09–4.20	2.08±0.73	1.30–4.20	2.43±0.95	1.09–3.00	1.97±0.67	4.95						
DbA	0.49–6.89	1.86±0.98	2.19–6.06	3.36±1.27	1.90–3.39	2.72±0.50	2.48						
InP	1.90–6.06	3.00±0.88	1.22–6.89	2.58±1.58	1.17–2.51	1.69±0.50							
BgP	1.69–4.99	2.77±0.72	1.69–4.75	2.82±0.94	1.76–3.25	2.55±0.38	9.06						
<i>T-PAH</i>	<i>15.16–45.49</i>	<i>27.39±7.63</i>	<i>16.66–45.49</i>	<i>28.28±8.35</i>	<i>15.16–29.66</i>	<i>23.68±4.17</i>	<i>44.2</i>	<i>5.1</i>	<i>11.6</i>	<i>33.0</i>	<i>36.33</i>	<i>34.82</i>	
LMW			1.70–3.71	2.38±0.58	1.40–2.70	2.07±0.33							
MMW			2.69–11.54	6.70±2.38	2.86–11.86	6.93±3.25							
HMW			10.89–34.70	19.20±7.57	9.11–19.46	14.68±3.29							

The italic data implied the total concentrations of PAHs

^aThis study

^bThe urban site in China from 31 December 2007 to 12 January 2008 and the ΣPAHs include 14 PAH compounds, including the concentration of PerY which is 1.04 ng/m³, and the total concentration of BkF and BbF is 5.38 ng/m³ (Tan et al. 2011)

^cThe rural site in Lampang province, Northern Thailand, from 9 March to 12 March 2009 and the ΣPAHs include 16 PAH compounds (Phoothiwut et al. 2013)

^dThe suburban site in Brazil in August 2002 and September 2003 and the ΣPAHs include 16 PAH compounds (De Andrade et al. 2010)

^eThe rural site in China in October and December in 2005 and the ΣPAHs include 21 PAH compounds (Lai et al. 2009)

^fThe rural field in Taiyuan from April 2010 to March 2011 by medium-volume (200–400 l/min) cascade impactors for 72 h and the ΣPAHs include 21 PAH compounds (Li et al. 2014)

^hThe rural site in Henan, every 3 days during autumn (Sep to Oct 2012) and the ΣPAHs include 16 PAH compounds from coal combustion (Wu et al. 2015)

concentration of the 12 PAHs. During non-haze episodes, the concentration of COMPAHs was $19.91 \pm 3.99 \text{ ng m}^{-3}$, accounting for $83.79 \pm 3.15 \%$ of the 12 PAHs. The high proportion of COMPAHs indicates that combustion sources are the leading contributors during both haze and non-haze episodes, which is supported by the significantly positive correlations between COMPAHs and the 12 PAHs ($R=0.98$) (Fig. 2). The LMW/HMW ratio is often considered to be an index for distinguishing pyrogenic from petrogenic sources. The negative correlation ($R=-0.66$) found between the LMW/HMW ratio and the COMPAH concentration (Fig. 2) confirms that the predominant source of PAHs at Yucheng was from combustion.

Generally, specific PAHs, such as BaA, BbF, BkF, BaP, InP, and DbA, are chosen to evaluate the carcinogenic potential of PAHs in a given region. The concentrations of these species fluctuated in the range of $18.35 \pm 7.26 \text{ ng m}^{-3}$ ($64.91 \pm 9.75 \%$) of the 12 PAHs total concentration during haze episodes and $13.71 \pm 3.17 \text{ ng m}^{-3}$ ($57.9 \pm 10.25 \%$) during non-haze episodes, respectively. The toxicity and carcinogenic risk of the measured PAHs are further analysed in the section focusing on cancer risk assessment.

PAH source identification

Principal component analysis

Principal component analysis (PCA) with varimax rotation was used to identify the sources of PAHs during both haze and non-haze episodes at Yucheng (Table 2). Three principal components (PCs) were extracted, which accounted for more than 88.71 % of the total variance.

PC1 accounted for 51.29 % of the total variance and was dominated by BaA, Chr, BbF, and BkF. The higher levels of BkF, BbF, and BaA are indicative of the influence of diesel and gasoline emissions (Larsen and Baker 2003; Venkataraman et al. 1994; Dong and Lee 2009). and Chr is a tracer of coal

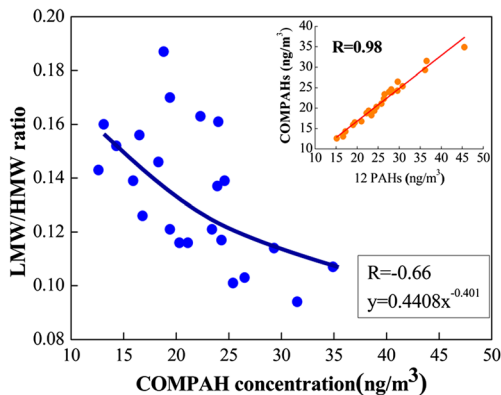


Fig. 2 Relationship between COMPAH concentration and LMW/HMW ratio; relationship between COMPAH and 12 PAH concentrations

Table 2 PCA result for all day and night particulate PAH compounds at Yucheng

PAH	PC1	PC2	PC3
Phe	0.062	<i>0.949</i>	-0.019
Ant	-0.029	0.100	<i>0.909</i>
Flt	0.201	-0.198	<i>0.881</i>
Pyr	-0.056	-0.175	<i>0.909</i>
Chr	<i>0.930</i>	0.109	0.089
BaA	<i>0.955</i>	0.026	0.143
BkF	<i>0.892</i>	0.365	-0.076
BbF	<i>0.808</i>	0.337	-0.186
BaP	0.412	<i>0.816</i>	-0.270
InP	0.604	<i>0.772</i>	-0.029
DbA	0.182	<i>0.914</i>	-0.136
BgP	0.712	<i>0.551</i>	0.258
Explained variance (%)	<i>51.29</i>	<i>24.09</i>	<i>13.33</i>

The italicized data implied major PAH compounds in corresponding principal component. Extraction method: principal component analysis. Rotation method: varimax with Kaiser normalization

combustion (Harrison et al. 1996). Thus, PC1 appeared to be a mixture of coal combustion and vehicle emissions. PC2 (24.09 % of the total variance) was dominated by Phe, BaP, InP, and DbA with a moderate loading for BgP, which are typical markers of vehicle emissions (Harrison et al. 1996). PC3, accounting for 13.33 % of the total variance, was highly dominated by Ant, Flt, and Pyr, which are tracers of fossil fuel combustion of liquefied gas, natural gas, and coal (Ilias and Euripides 2002). Some researchers have also reported that Ant, Flt, and Pyr can be attributed to biomass burning (Oros 2006). Additionally, HMW and other stable molecular PAHs are preferentially formed in high temperature, and LMW-PAHs are generally formed during low-temperature reaction processes, such as biomass burning (Mostert et al. 2010). Therefore, PC3 should be attributed to biomass burning and fossil fuel combustion. Overall, the results obtained from PCA revealed that fossil fuel combustion, vehicle emissions, and coal and biomass burning are likely the dominant sources of PAHs at Yucheng in summer.

Diagnostic ratio

The possible sources of PAHs may be identified by the isomer ratios of Ant/(Ant+Phe), BaA/(BaA+Chr), Flt/(Flt+Pyr), and InP/(InP+BgP) to discriminate between petrogenic and pyrolytic sources (shown in Table 3, Zhang et al. 2006). As shown in Fig. 3a, the ratios of BaA/(BaA+Chr) in non-haze (0.64–0.81) and haze (0.63–0.80) episodes were all higher than 0.35, indicating a pyrolytic source. The values of InP/(InP+BgP) ranged from 0.47–0.56 to 0.49–0.57 for non-haze and haze episodes, respectively, indicating a mixed source of

Table 3 Diagnostic ratios of particulate PAHs

	Reference source emissions	Reference
Ant/(Ant+Phe)	<0.1 petroleum >0.1 combustion	(Han et al. 2011)
Flt/(Flt+Pyr)	<0.4 petroleum source 0.4–0.5 liquid fossil fuel combustion >0.5 biomass and coal combustion	(Yunker et al. 2002)
BaA/(BaA+Chr)	<0.2 petrogenic 0.2–0.35 petrogenic or pyrolytic sources >0.35 pyrolytic sources	(Hu et al. 2012)
InP/(InP+BgP)	<0.2 petroleum and petrogenic sources 0.2–0.5 petroleum combustion(liquid fossil fuel, vehicle, and crude oil combustion) >0.5 contribution of coal, grass, and wood	(Yunker et al. 2002)

petroleum, coal, and biomass combustion. However, the 82 % of the ratios of Ind/(Ind+BgP) during the haze period were greater than 0.5, whereas only 57 % of the values during the non-haze were greater than 0.5, suggesting that a source of coal combustion and biomass burning was only dominant in

the hazy period (Khalili et al. 1995; Guo et al. 2003b). Furthermore, the distinction between PAH emission sources in non-haze and haze episodes is more clearly reflected in Fig. 3b, in which the scatter plot of the ratios Flt/(Flt+Pyr) and Ant/(Ant+Phe) clearly separates haze from non-haze PAHs. The results of Ant/(Ant+Phe) were higher than 0.1 during both the haze and non-haze periods, revealing the type of combustion source. Eighty-two percent of the sample ratios of Flt/(Flt+Pyr) were above 0.5 during the haze episodes, indicating that biomass or coal combustion was the main PAH source, and 64 % of the Flt/(Flt+Pyr) ratio was found to be between 0.4 and 0.5 during non-haze periods, revealing that petroleum combustion played a dominant role at this time. Overall, we can conclude that the main sources during both periods were pyrolytic, with coal and biomass combustion significantly contributing to haze episodes and liquid fossil fuel (petroleum) combustion dominantly contributing to non-haze episodes.

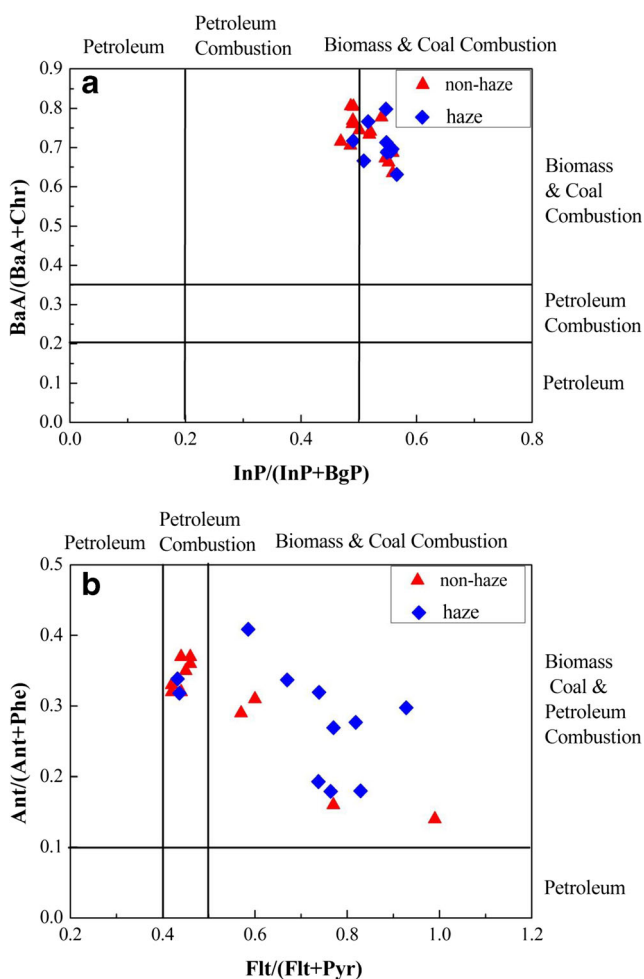


Fig. 3 Diagnostic ratios between InP/(InP+BgP) and BaA/(BaA+Chr) (a) and between Flt/(Flt+Pyr) and Ant/(Ant+Phe) (b)

Cancer risk assessment

Previously, the toxic equivalency factors (TEFs) for all known PAH species have been reported by Nisbet and LaGoy (1992), which reflects the carcinogenic properties of individual PAHs. On this list, BaP has been given a TEF of 1.0 (Nisbet and LaGoy 1992), and the concentrations of the individual PAHs are then converted to the BaP_{eq} concentrations based on the TEFs and the following equation (2). Table 4 shows the $\sum BaP_{eq}$ values obtained in this study.

$$\sum BaP_{eq} = \sum (PAH_i \times TEF_i) \quad (2)$$

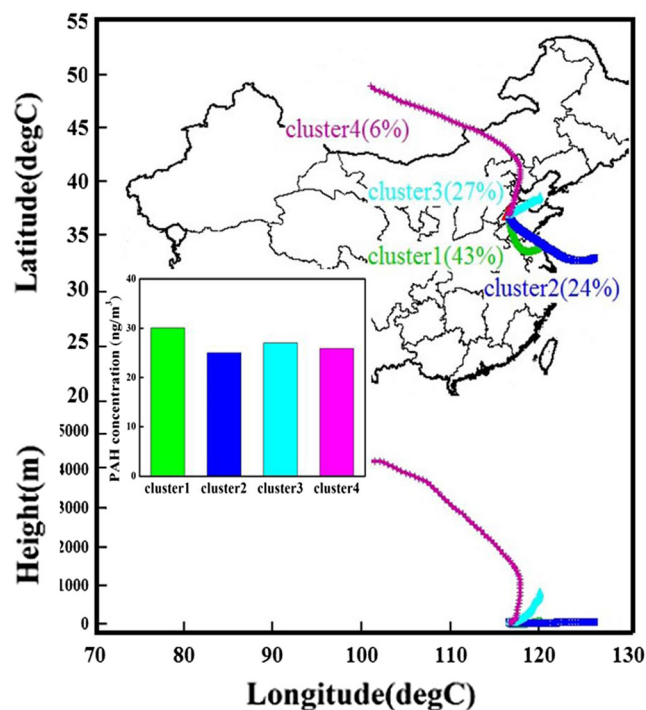
where PAH_i is the individual concentration of each PAH and TEF_i is the individual TEF of each PAH. Samples collected during the haze episodes exhibited a higher $\sum BaP_{eq}$ value (7.09 ng m^{-3}) than that in non-haze samples (5.64 ng m^{-3}). The $\sum BaP_{eq}$ values of PAH in haze and non-haze episodes were both lower than the national standard of 10 ng m^{-3}

Table 4 Health risk assessment for total BaP_{eq} by age-specific group

Exposure parameter	Unit	Infant	Toddler	Children	Adolescent	Adult	Adult
Exposure variable		0–1year	1–6years	6–12years	12–18years	18–30years	30–70years
Body weight (BW)	kg	7	15	31.2	38	66	66
Exposure frequency (EF)	dayyear ⁻¹	350	350	350	350	350	350
Exposure duration (ED)	years	1	5	6	6	12	40
Inhalation rate IR _{inhalation}	m ³ day ⁻¹	5.4	9	12	15.7	15.7	15.7
Average life span (ALT)	years	70	70	70	70	70	70
Samples	Mean of \sum BaP _{eq} (ng/m ³)	Infant	Toddler	Children	Adolescent	Adult	Adult
ILCR		0–1year	1–6years	6–12years	12–18years	18–30years	30–70years
Non-haze	5.64	1.87E-07	7.28E-07	5.60E-07	6.01E-07	6.93E-07	2.31E-06
Haze	7.09	2.35E-07	9.15E-07	7.04E-07	7.56E-07	8.71E-07	2.90E-06
Total risk		1year	6years	12years	18years	30years	70years
Non-haze		1.87E-07	9.15E-07	1.47E-06	2.08E-06	2.77E-06	5.08E-06
Haze		2.35E-07	1.15E-06	1.85E-06	2.61E-06	3.48E-06	6.38E-06

(Zhu et al. 2013) but were significantly higher than the World Health Organization standard (1 ng m⁻³) (Ventafriidda et al. 1987).

In this study, a probabilistic risk assessment framework was applied to estimate the cancer risk incurred from exposure routes to PAHs via inhalation. Probabilistic risk assessment for personal exposure to carcinogenic PAHs showed that an ILCR between 10⁻⁶ and 10⁻⁴ indicates a potential risk, whereas an ILCR greater than 10⁻⁴ denotes a high potential health risk (Liao and Chiang 2006). The acceptable level is equal to or less than 10⁻⁶ (Chiang et al. 2009). The estimated ILCR values for each age-specific group are listed in Table 4. For all the age-specific groups, the ILCR and the total risk values for haze were approximately 1.4 times higher than those for non-haze periods, revealing a higher probabilistic risk during the haze periods when compared with non-haze periods. The ILCR values increased as the age bracket increased from infant to adult (30–70 years old), except for the toddler age group. The ILCR values for non-haze (7.28E-07) and haze (9.15E-07) episodes for toddlers are both higher than those for the corresponding 18–30-year-old adults (non-haze, 6.93E-07; haze, 8.71E-07), indicating that although the exposure time for toddlers is less than 6 years, the health risk is still higher than that for 18–30-year-old adults. The values obtained in our study show that the highest estimated ILCR values are 2.31E-06 (in non-haze) and 2.90E-06 (in haze) for adult residents (30–70 years old), suggesting that adults over

**Fig. 4** Mean 3-day backward trajectory clusters during sampling periods from 1 to 30 June

30 years old may be at risk of developing cancer and that the risk in the other age groups is within acceptable levels. Additionally, the total accumulated risk worsens as the age increases from infant (1 year old) to adult (70 years old) in both non-haze and haze conditions, and the highest estimated cancer risk values calculated were $5.08E-06$ (in non-haze) and $6.38E-06$ (in haze) for elderly adult residents (70 years old).

Influence of back trajectories of air mass transport

To better understand the long-distance transport of pollutants during the sampling period, the HYSPLIT model was used to calculate 72-h back trajectories every 2 h at 50 m above ground level. The air mass trajectories at Yucheng were classified into four clusters.

Figure 4 shows that the cluster with the highest frequency (cluster 1) comprised 43 % of the total trajectories, which originated in eastern Jiangsu province and then passed over the border between Jiangsu and Anhui provinces before arriving in Yucheng. The air masses associated with this cluster moved slowly at an altitude of between 0 and 100 m, indicating that the air pollutants were influenced by ground layer pollution. The highest concentrations (30.46 ng m^{-3}) of PAHs were found to correspond with this cluster. Fu et al. (2012) reported that intensive biomass burning is usually concentrated in the region of Shandong, Jiangsu, and Anhui provinces in June. It is likely that these areas greatly contribute to the concentrations of PAHs downwind. Cluster 3, which contained the second highest concentrations of PAHs (27.55 ng m^{-3}) and accounted for 27 % of the total trajectories, originated in the Bohai Gulf and travelled along the border of Hebei and Shandong provinces. The Bohai economic zone, which is one of the most populated and industrial zones in China, has been reported to exhibit elevated emissions of PAHs (Zhang et al. 2009). Hence, long-distance transport of sources of industrial pollution and biomass burning contributed significantly to the concentrations of PAHs in Yucheng.

Conclusions

The characteristics of 12 $\text{PM}_{2.5}$ -bound PAHs were investigated during haze and non-haze episodes at Yucheng in June 2013. The total average concentration of the 12 PAH species during haze episodes was $28.28 \pm 8.35 \text{ ng m}^{-3}$, which was higher than the average concentration measured during non-haze episodes ($23.68 \pm 4.17 \text{ ng m}^{-3}$). In order to analyse the compositional pattern of PAHs during non-haze and haze episodes, the 12 PAHs were classified into LMW, MMW, and HMW species and as COMPAHs and carcinogenic PAHs. The results showed that COMPAHs and HMW-PAHs accounted for a substantial portion in the 12 PAHs, which signified that the dominant sources of PAHs at Yucheng

during both non-haze and haze periods were from combustion processes. Moreover, the proportion of HMW-PAHs increased from 62.3 % in non-haze to 67.9 % in haze episodes. Diagnostic ratios and PCA, which were used to identify the sources of the PAHs, indicated that vehicle emissions, fossil fuel combustion, coal combustion, and biomass burning were the main sources of PAHs during the sampling period. Coal combustion and biomass burning were determined to be the dominant contributors to PAHs during haze episodes, and liquid fossil fuel (petroleum) combustion was the dominant source during non-haze episodes. Additionally, the $\Sigma\text{BaP}_{\text{eq}}$ and ILCR values of PAHs were calculated to estimate the toxicity and the carcinogenic risk of PAHs to human health. The BaP_{eq} value for haze samples (7.09 ng m^{-3}) was higher than that for non-haze samples (5.64 ng m^{-3}) revealing the stronger toxicity during haze episodes, and the ILCR results showed that adults over 30 years old are at an elevated risk of cancer. The calculated cancer risk for the other age groups was found to be within the acceptable levels. Finally, on the basis of back-trajectory analysis, we conclude that the long-distance transport of industrial pollution from the Bohai Gulf region and pollution emitted from biomass burning in the southeastern provinces of Shandong, Anhui, and Jiangsu is a significant source of PAHs at Yucheng.

Acknowledgements The funding of this research was supported by the Taishan Scholar Grant (ts20120552), the National Natural Science Foundation of China (Nos. 21307074 and 21577079), and the Fundamental Research Funds of Shandong University (No. 2014GN010).

References

- Cao GL, Zhang XY, Wang YQ, Zheng FC (2008) Estimation of emissions from field burning of crop straw in China. *Chin Sci Bull* 53: 784–790
- Chen SC, Liao CM (2006) Health risk assessment on human exposed to environmental polycyclic aromatic hydrocarbons pollution sources. *Sci Total Environ* 366:112–123
- Chiang KC, Chio CP, Chiang YH, Liao CM (2009) Assessing hazardous risks of human exposure to temple airborne polycyclic aromatic hydrocarbons. *J Hazard Mater* 166:676–685
- China, Ministry of Environmental Protection of The People's Republic of China (2012) Ambient air quality standards (GB3095-2012, in Chinese). Available from: <http://www.chinacsrmap.org/>
- De Andrade SJ, Cristale J, Silva FS, Zocolo GJ, Marchi MRR (2010) Contribution of sugar-cane harvesting season to atmospheric contamination by polycyclic aromatic hydrocarbons (PAHs) in Araraquara city, Southeast Brazil. *Atmos Environ* 44:2913–2919
- Dong TTT, Lee BK (2009) Characteristics, toxicity, and source apportionment of polycyclic aromatic hydrocarbons (PAHs) in road dust of Ulsan, Korea. *Chemosphere* 74:1245–1253
- Duan JC, Guo SJ, Tan JH, Wang SL, Chai FH (2012) Characteristics of atmospheric carbonyls during haze days in Beijing, China. *Atmos Res* 114:17–27
- Fang M, Zheng M, Wang F, To KL, Jaafar AB, Tong SL (1999) The solvent-extractable organic compounds in the Indonesia biomass

- burning aerosols-characterization studies. *Atmos Environ* 33:783–795
- Fu PQ, Kawamura K, Chen J, Li J, Sun YL, Liu Y et al (2012) Diurnal variations of organic molecular tracers and stable carbon isotopic composition in atmospheric aerosols over Mt. Tai in the North China Plain: an influence of biomass burning. *Atmos Chem Phys* 12:8359–8375
- Guo H, Lee SC, Ho KF, Wang XM, Zou SC (2003a) Particle-associated polycyclic aromatic hydrocarbons in urban air of Hong Kong. *Atmos Environ* 37:5307–5317
- Guo ZG, Sheng LF, Feng JL, Fang M (2003b) Seasonal variation of solvent extractable organic compounds in the aerosols in Qingdao, China. *Atmos Environ* 37:1825–1834
- Han B, Ding X, Bai ZP, Kong SF, Guo GH (2011) Source analysis of particulate matter associated polycyclic aromatic hydrocarbon (PAHs) in an industrial city in northeastern China. *J Environ Monitor* 13:2597–2604
- Harrison RM, Smith DJT, Luhana L (1996) Source apportionment of atmospheric polycyclic aromatic hydrocarbons collected from an urban location in Birmingham, UK. *Environ Sci Technol* 30:825–832
- Hassanien MA, Abdel-Latif NM (2008) Polycyclic aromatic hydrocarbons in road dust over Greater Cairo, Egypt. *J Hazard Mater* 151:247–254
- Hu J, Liu CQ, Zhang GP, Zhang YL (2012) Seasonal variation and source apportionment of PAHs in TSP in the atmosphere of Guiyang, Southwest China. *Atmos Res* 118:271–279
- Ilias GK, Euripides GS (2002) Particle size distribution of organic primary and secondary aerosol constituents in urban, background marine, and forest atmosphere. *J Geophys Res* 107:1–12
- Khalili NR, Scheff PA, Holsen TM (1995) PAH source fingerprints for coke ovens, diesel and gasoline engines, highway tunnels, and wood combustion emissions. *Atmos Environ* 29:533–542
- Koe LCC, Arellano AF, McGregor JL (2001) Investigating the haze transport from 1997 biomass burning in Southeast Asia: its impact upon Singapore. *Atmos Environ* 35:2723–2734
- Lai CH, Chen KS, Wang HK (2009) Influence of rice straw burning on the levels of polycyclic aromatic hydrocarbons in agricultural county of Taiwan. *J Environ Sci* 21:1200–1207
- Larsen RK, Baker JE (2003) Source apportionment of polycyclic aromatic hydrocarbons in the urban atmosphere: a comparison of three methods. *Environ Sci Technol* 37:1873–1881
- Li WJ, Shao LY, Buseck PR (2010) Haze types in Beijing and the influence of agricultural biomass burning. *Atmos Chem Phys* 10:8119–8130
- Li W, Wang C, Wang HQJ, Chen JW, Shen HZ, Shen GF et al (2014) Atmospheric polycyclic aromatic hydrocarbons in rural and urban areas of northern China. *Environ Pollut* 192:83–90
- Liao CM, Chiang KC (2006) Probabilistic risk assessment for personal exposure to carcinogenic polycyclic aromatic hydrocarbons in Taiwanese temples. *Chemosphere* 63:1610–1619
- Ma WL, Li YF, Qi H, Sun DZ, Liu LY, Wang DG (2010) Seasonal variations of sources of polycyclic aromatic hydrocarbons (PAHs) to a northeastern urban city, China. *Chemosphere* 79:441–447
- Mostert MMR, Ayoko GA, Kokot S (2010) Application of chemometrics to analysis of soil pollutants. *Trends Anal Chem* 29:430–435
- Mu Q, Zhang SQ (2013) The economic cost evaluation of haze event in China. Available from: <http://www.paper.edu.cn/releasepaper/content/05-493>
- Nisbet IC, LaGoy PK (1992) Toxic equivalency factors (TEFs) for polycyclic aromatic hydrocarbons (PAHs). *Regul Toxicol Pharmacol* 16:290–300
- Oros DR (2006) Identification and emission factors of molecular tracers in organic aerosols from biomass burning: part 3. Grasses. *Appl Geochem* 21:919–940
- Peng C, Chen WP, Liao XL, Wang ME, Ouyang ZY, Jiao WT et al (2011) Polycyclic aromatic hydrocarbons in urban soils of Beijing: status, sources, distribution and potential risk. *Environ Pollut* 159:802–808
- Phoothiwut S, Junyapoon S (2013) Size distribution of atmospheric particulates and particulate-bound polycyclic aromatic hydrocarbons and characteristics of PAHs during haze period in Lampang Province, Northern Thailand. *Air Qual Atmos Health* 6:397–405
- Shen G, Zhang Y, Wei S, Chen YC, Yang CL, Lin PC et al (2014) Indoor/outdoor pollution level and personal inhalation exposure of polycyclic aromatic hydrocarbons through biomass fuelled cooking. *Air Qual Atmos Health* 7:449–458
- Sierra MR, Rosazza NG, Préndez M (2005) Polycyclic aromatic hydrocarbons and their molecular diagnostic ratios in urban atmospheric respirable particulate matter. *Atmos Res* 75:267–281
- Tan JH, Guo SJ, Ma YL, Duan JC, Cheng Y, He KB, Yang F (2011) Characteristics of particulate PAHs during a typical haze episode in Guangzhou, China. *Atmos Res* 102:91–98
- USEPA (United States Environmental Protection Agency) (2005) Guidelines for carcinogenic risk assessment. Available from: http://www.epa.gov/raf/publications/pdfs/CANCER_GUIDELINES_FINAL_3-25-05PDF. Accessed November 2013
- Venkataraman C, Lyons JM, Friedlander SK (1994) Size distributions of polycyclic aromatic hydrocarbons and elemental carbon 1 Sampling, measurement methods, and source characterization. *Environ Sci Technol* 28:555–562
- Ventafriida V, Tamburini M, Caraceni A, De Conno F, Naldi F (1987) A validation study of the WHO method for cancer pain relief. *Cancer* 59:850–856
- Wang Y, Zhuang GS, Sun Y, An ZS (2006) The variation of characteristics and formation mechanisms of aerosols in dust, haze, and clear days in Beijing. *Atmos Environ* 40:6579–6591
- Watson JG (2002) Visibility: science and regulation. *J Air Waste Manage Assoc* 52:628–713
- Wen L, Chen JM, Yang LX, Wang XF, Xu CH, Sui X et al (2015) Enhanced formation of fine particulate nitrate at a rural site on the North China Plain in summer: the important roles of ammonia and ozone. *Atmos Environ* 101:294–302
- Wu SP, Tao S, Xu FL, Dawson R, Lan T, Li BG, Cao J (2005) Polycyclic aromatic hydrocarbons in dustfall in Tianjin, China. *Sci Total Environ* 345:115–126
- Wu F, Liu XP, Wang W, Yu BM, Chan CY, Liu WX et al (2015) Characterization of particulate-bound PAHs in rural households using different types of domestic energy in Henan Province, China. *Sci Total Environ* 536:840–846
- Xu FL, Qin N, Zhu Y, HeW KXZ, Barbour MT et al (2013a) Multimedia fate modeling of polycyclic aromatic hydrocarbons (PAHs) in Lake Small Baiyangdian, Northern China. *Ecol Model* 252:246–257
- Xu WZ, Chen H, Li DH, Zhao FS, Yang Y (2013b) A case study of aerosol characteristics during a haze episode over Beijing. *Procedia Environ Sci* 18:404–411
- Yan XY, Ohara T, Akimoto H (2006) Bottom-up estimate of biomass burning in mainland China. *Atmos Environ* 40:5262–5273
- Yang SJ, He HP, Lu SL, Chen D, Zhu JX (2008) Quantification of crop residue burning in the field and its influence on ambient air quality in Suqian, China. *Atmos Environ* 42:1961–1969
- Yunker MB, Macdonald RW, Vingarzan R, Mitchell RH, Goyette D, Sylvestre S (2002) PAHs in the Fraser River basin: a critical appraisal of PAH ratios as indicators of PAH source and composition. *Org Geochem* 33:489–515
- Zhang Q, Streets DG, Carmichael GR, He KB, Huo H, Kannari A et al (2009) Asian emissions in 2006 for the NASA INTEX-B mission. *Atmos Chem Phys* 9:5131–5153
- Zhang YX, Tao S (2009) Global atmospheric emission inventory of polycyclic aromatic hydrocarbons (PAHs) for 2004. *Atmos Environ* 43:812–819

- Zhang YX, Tao S, Cao J, Coveney RM (2007) Emission of polycyclic aromatic hydrocarbons in China by county. *Environ Sci Technol* 41: 683–687
- Zhang HB, Luo YM, Wong MH, Zhao QG, Zhang GL (2006) Distributions and concentrations of PAHs in Hong Kong soils. *Environ Pollut* 141:107–114
- Zhou JB, Wang TG, Huang YB, Mao T, Zhong NN (2005) Size distribution of polycyclic aromatic hydrocarbons in urban and suburban sites of Beijing, China. *Chemosphere* 61:792–799
- Zhu YH, Yang LX, Yuan Q, Yan C, Dong C, Meng CP et al (2013) Airborne particulate polycyclic aromatic hydrocarbon (PAH) pollution in a background site in the North China Plain: concentration, size distribution, toxicity and sources. *Sci Total Environ* 466–467:357–368
- Zhu YH, Yang LX, Meng CP, Yuan Q, Yan C, Dong C et al (2015) Indoor/outdoor relationships and diurnal/nocturnal variations in water-soluble ion and PAH concentrations in the atmospheric PM_{2.5} of a business office area in Jinan, a heavily polluted city in China. *Atmos Res* 153:276–285